IEEE Access
Multidisciplinary | Rapid Review | Open Access Journal

Received 20 November 2024, accepted 9 December 2024, date of publication 11 December 2024,
date of current version 19 December 2024.

Digital Object Identifier 10.1109/ACCESS.2024.3515895

RESEARCH ARTICLE

IoUT-Oriented an Efficient CNN Model for Modulation Schemes Recognition in Optical Wireless Communication Systems

M. MOKHTAR ZAYED[1,2], SAEED MOHSEN[3,4], ABDULLAH ALGHURIED[5], HASSAN HIJRY[5], (Associate Member, IEEE), AND MONA SHOKAIR[2,6]

[1]Department of Communications and Computers Engineering, Higher Institute of Engineering, El-Shorouk Academy, Al Shorouk City 11837, Egypt
[2]Department of Communications, Faculty of Electronic Engineering, Menoufia University, Minuf 32951, Egypt
[3]Department of Electronics and Communications Engineering, Al-Madinah Higher Institute for Engineering and Technology, Giza 12947, Egypt
[4]Department of Artificial Intelligence Engineering, Faculty of Computer Science and Engineering, King Salman International University (KSIU), El-Tor 46511, Egypt
[5]Department of Industrial Engineering, Faculty of Engineering, University of Tabuk, Tabuk 47512, Saudi Arabia
[6]Department of Electrical Engineering, Faculty of Engineering, October 6 University, Giza Governorate, 6th of October City 12585, Egypt

Corresponding author: Saeed Mohsen (g17082131@eng.asu.edu.eg)

ABSTRACT The rapid advancement of the Internet of Underwater Things (IoUT) necessitates robust, high-capacity communication systems that can operate efficiently in the challenging conditions of underwater environments. Optical Wireless Communication (OWC) systems, leveraging the advantages of high data rates and low latency, offer a compelling solution for IoUT. However, accurate modulation recognition in these systems remains a significant challenge due to the variable nature of underwater channels. This paper explores the application of Convolutional Neural Networks (CNNs) for modulation recognition in the OWC systems, focusing specifically on 64-QAM (Quadrature Amplitude Modulation) and 32-PSK (Phase Shift Keying). A CNN model-based approach is proposed to automatically extract and classify modulation features from received signals, demonstrating superior performance compared to traditional recognition methods. The model is applied to a dataset of 626 simulated images, categorized into two modulation types: 64QAM and 32PSK. Keras and TensoFlow frameworks are used to implement the model, the CNN undergoes hyperparameter tuning and data augmentation to optimize accuracy. The model's performance is assessed using a confusion matrix, along with precision-recall (PR) and receiver operating characteristic (ROC) curves. The experimental results show that the CNN achieves high accuracy in recognizing modulation types, with a testing accuracy of 100% and a testing loss rate of 1.82×10^{-6}. Additionally, the model records a Precision, Recall, F1-score, and area under the ROC of 100%. The experiments reveal that the CNN model achieves high accuracy in differentiating between 64-QAM and 32-PSK under varying underwater conditions, highlighting its potential for enhancing IoUT communication reliability.

INDEX TERMS Deep learning, convolutional neural networks (CNN), modulation recognition, 64-QAM, 32-PSK, optical wireless communications (OWC), Internet of Underwater Things (IoUT).

I. INTRODUCTION

The rapid development of the Internet of Underwater Things (IoUT) has ushered in a new era of underwater communication networks, enabling a wide range of applications such as environmental monitoring, underwater exploration, and resource management [1], [2], [3]. OWC systems have emerged as a promising technology to support high-speed data transmission in underwater environments, offering advantages over traditional acoustic and radio frequency (RF) communication systems, including higher bandwidth and lower latency [4], [5]. However, the complex and dynamic

The associate editor coordinating the review of this manuscript and approving it for publication was Ines Domingues.

nature of underwater environments poses significant challenges to the reliable transmission of optical signals. Factors such as water absorption, scattering, and turbulence make it difficult to maintain high data rates and low error probabilities. In this context, modulation recognition plays a critical role in ensuring the integrity and efficiency of communication systems. Automatic Modulation Recognition (AMR) is a key technique that allows the receiver to recognize the modulation scheme of the received signal without prior knowledge, thereby facilitating adaptive demodulation and improving overall system performance [6], [7], [8], [9]. Despite the progress in OWC systems, the inherent challenges of underwater environments, combined with the increasing complexity of modulation schemes, demand more advanced recognition techniques. Traditional methods for modulation recognition, such as likelihood-based approaches and feature-based classifiers, often fall short in underwater scenarios due to their sensitivity to noise and channel impairments. These limitations have motivated the exploration of deep learning-based methods, which have shown remarkable success in various domains, including image and speech recognition [10].

Convolutional Neural Networks (CNNs), in particular, have demonstrated strong capabilities in feature extraction and pattern recognition, making them a promising solution for AMR in optical wireless communication systems [11], [12], [13]. The problem statement addressed in this paper is the need for a robust and efficient modulation recognition technique capable of accurately identifying complex modulation schemes in challenging underwater environments. Specifically, the focus is on two widely used modulation formats: 64-QAM and 32-PSK. These modulation schemes offer high spectral efficiency, making them suitable for IoUT applications where bandwidth is limited. However, their complexity also makes them more susceptible to errors in the presence of noise and distortion, underscoring the need for advanced recognition techniques.

The objective of this study to address the critical challenge of modulation recognition in underwater optical wireless communication systems (UOWCs) by introducing a deep learning-based solution. The findings are expected to contribute to the advancement of IoUT technologies, enabling more reliable and efficient underwater communication networks. Thus, the paper aims to develop a deep learning-based approach for modulation identification in OWC systems, with a particular emphasis on 64-QAM and 32-PSK modulation schemes. By leveraging the powerful feature extraction capabilities of CNNs, the proposed method aims to enhance the accuracy and robustness of modulation recognition in underwater environments.

The main contributions of this paper are fivefold:

- A comprehensive analysis of the challenges associated with modulation recognition in underwater optical communication systems, highlighting the limitations of traditional methods.
- The design and implementation of a CNN-based model tailored to the specific characteristics of 64-QAM and 32-PSK modulation schemes, incorporating techniques to enhance robustness against underwater channel impairments.
- A detailed evaluation of the proposed model's performance was conducted through simulations using various measures based on a dataset of 626 simulated images of the modulation.
- A discussion on the potential applications of the proposed approach in IoUT, including its integration into adaptive communication systems for real-time modulation recognition and decision-making.
- Comparing the results achieved by the proposed CNN with several state-of-the-art methods and demonstrating its effectiveness in reducing bit error rates and enhancing signal-to-noise ratios.

The remainder of this paper is organized as follows: Section II provides a comprehensive literature review of existing works related to a CNN deep learning-based modulation identification. Section III presents the applications in optical wireless communications, specifically in IoUT environments. Section IV presents the proposed methodology, including the system model used in this study, detailing the key components of the OWC system, the modulation schemes under consideration, and describing the deep learning framework and the CNN architecture employed for modulation recognition. Section V presents the results, while the discussion is introduced in Section VI, where the performance of the proposed method is evaluated and compared against traditional approaches. Finally, Section VII concludes the paper, summarizing the key results and discussing potential directions for future research.

II. RELATED WORK

In the literature, different modulation techniques are used to optimize communication. For instance, 64-QAM (Quadrature Amplitude Modulation) is a method that allows the transmission of multiple bits per symbol by varying both amplitude and phase, offering high spectral efficiency but at the cost of increased sensitivity to noise and channel impairments. Conversely, 32-PSK (Phase Shift Keying) modulates the phase of the carrier signal to represent data, striking a balance between spectral efficiency and robustness to noise, which is particularly beneficial in challenging underwater environments.

Traditional methods for modulation recognition typically rely on statistical features and machine learning (ML) classifiers, requiring manual feature extraction that may struggle to capture the complex patterns found in underwater channels [10], [14], [15]. To overcome these limitations, Convolutional Neural Networks (CNNs) have been increasingly utilized due to their ability to learn hierarchical feature representations directly from raw data [11], [12], [13].

This automatic feature extraction makes CNNs particularly effective for modulation recognition in OWC systems,

enabling more accurate and robust identification of modulation schemes like 64-QAM and 32-PSK in the presence of underwater challenges. Optical Wireless Communication (OWC) systems provide high data rates and secure transmission, making them ideal for IoUT applications. However, the performance of OWC systems is often challenged by the underwater environment, where factors such as signal attenuation due to absorption and scattering, as well as fluctuations caused by turbulence, can significantly impact signal quality [16], [17], [18]. Our research paper presents an extensive review of the literature in this field, detailed as follows:

The study in [19] focused on enhancing modulation classification in underwater optical wireless communication (UOWC) systems, a critical aspect of the emerging IoUT. Given the challenges of constrained data transfer and frequent transmission failures in underwater environments, the study proposed the use of a Convolutional Neural Network (CNN) for classifying modulation schemes by transforming modulated signals into constellation images. Specifically, SqueezeNet, a compact and low-resource deep learning model, is employed to address the unique demands of UOWC systems. The simulation results demonstrated that SqueezeNet offers accurate and efficient modulation classification, improving the reliability and data rates of UOWC systems, making it suitable for IoUT applications such as underwater exploration and data transmission.

In [20], the authors focused on developing an algorithm to extract a novel one-dimensional (1D) phase-related feature from received signals for automatic modulation classification (AMC). By using a CNN to learn and classify these features, they demonstrated that the 1D feature contains more intrinsic information about the modulation patterns compared to conventional features.

The algorithm's effectiveness is further validated through simulations, showing that the proposed system achieved a classification accuracy beyond 99% at 0 dB, outperforming traditional methods. Additionally, a comparison with two-dimensional (2D) constellation graph-based classification confirms the superiority of the proposed 1D feature extraction method.

The authors of [21] introduced a novel modulation classification method that leverages higher-order cumulants (HOCs) in combination with a decision tree (DT) classifier to enhance the recognition of modulation schemes, such as PSK and QAM, even at low signal-to-noise ratios (SNR). The method applied a threshold algorithm to sub-classifiers, each utilizing a single feature, to individually distinguish modulation types.

The study examined 1,000 signals across SNR values from -5 dB to 30 dB, achieving classification accuracies between 88% and 100% for various PSK and QAM schemes. The proposed classifier demonstrated superior accuracy and computational efficiency compared to existing methods, particularly due to the use of optimized logarithmic features, making it a highly effective solution for AMC.

In 2023, the authors of [22] explored the use of a voting-based deep CNN for automatic modulation classification (AMC) of M-QAM and M-PSK signals in wireless communication systems. The VB-DCNN extracted features from input signals passed through fading channels with additive white Gaussian noise (AWGN) and performed classification by combining predictions from several network instances trained on various data subsets. The proposed model demonstrated 99.2% accuracy at lower SNRs, outperforming existing state-of-the-art techniques. The study also suggested that increasing the network's layers can further enhance classification accuracy, and future improvements could focus on developing CNN-based classifiers optimized for resource-constrained environments.

Ref. [23] introduced SCGNet, a CNN designed for efficient and robust modulation identification in intelligent communication receivers. SCGNet featured a combination of sparse convolutional layers, including depthwise and grouped convolutions, to balance high recognition accuracy with low computational complexity.

The architecture incorporated three main modules: Generic Feature Extraction (GFE), Speed-Accuracy Tradeoff (SAT), and Deep Feature Extraction and Processing (DFEP). Experimental results using the RadioML2018.01A dataset showed that SCGNet achieved approximately 95.5% recognition accuracy at $+30$ dB SNR, outperforming existing methods while maintaining a compact model with fewer learnable parameters. The design of SCGNet made it well-suited for edge-based communication systems where both accuracy and efficiency are critical.

According to [24], the study introduced FiF-Net, a novel CNN designed for accurate modulation classification using constellation diagrams. FiF-Net employed multiple processing blocks with grouped and asymmetric convolutional layers organized in a flow-in-flow structure to effectively learn key radio characteristics from grayscale constellation images.

The network architecture incorporated skip connections to mitigate the vanishing gradient problem and preserve information. Extensive simulations on a dataset of eight digital modulation formats demonstrated that FiF-Net achieves approximately 87% classification accuracy at 0 dB SNR under multipath Rayleigh fading, surpassing several state-of-the-art models in constellation-based modulation classification.

In [25], This study introduced a generative adversarial network (GAN)-based signal inpainting method to address the challenge of missing samples in time-domain signals for automatic modulation classification (AMC). By restoring up to 50% of missing samples while preserving the global structure of each modulation type, the proposed method enhanced the accuracy of modulation classification. Experiments using the RadioML dataset showed that the GAN-based inpainting significantly improved classification accuracy compared

to state-of-the-art models without inpainting. The method effectively restored the characteristics of real signals, thereby enabling more accurate feature extraction for AMC. Future work will focus on validating the method with real-world data and optimizing its computational efficiency for practical deployment.

According to [26], the authors explored the use of CNNs to address performance issues in underwater optical wireless communication (UOWC) systems, particularly those caused by substantial attenuation and varying channel conditions. They introduced a modified CNN model designed to recover data from non-return to zero on–off keying (OOK-NRZ) modulated signals transmitted through Gulf seawater.

The CNN decoder significantly outperformed conventional fixed-threshold decoders (FTDs), achieving a bit error ratio (BER) reduction by about seven orders of magnitude, increasing the effective channel length by four times, and reducing the required SNR by approximately 20 dB. The CNN's robustness and performance improvements made it a promising alternative to traditional decoders, providing enhanced data recovery without needing prior channel knowledge.

The study in [27] explored the application of deep learning, specifically CNNs, to automatic modulation recognition in underwater acoustic communication. Unlike traditional ML methods that depend on manual feature extraction, CNNs automatically learn features directly from data, offering significant advantages. The study demonstrated that CNNs effectively recognize common underwater modulation methods, revealing their potential beyond image and language processing.

While the CNN approach showed promise in signal recognition and is expected to enhance applications in military and civilian underwater communication, the recognition performance under low SNR conditions still requires improvement. Future research should focus on optimizing deep learning techniques to better handle low-SNR scenarios.

In [28], This study reviewed the integration of deep learning (DL) with Automatic Modulation Recognition (AMR) in the context of 5G wireless communication systems. It began by outlining traditional AMR methods and their limitations, then highlights the advantages of applying deep learning algorithms to improve modulation recognition.

The paper provided a detailed examination of various deep learning techniques and their performance in AMR, especially in small sample environments. It also addressed the current challenges in this field and suggests future research directions. By summarizing recent advancements and comparing different approaches, the paper aims to offer valuable insights and references for further development in deep learning-based modulation recognition technologies.

As noted in [29], the study reviewed the advancements in AMR using deep learning techniques, highlighting their superior performance over traditional techniques in terms of recognition accuracy and false alarm rates. It covered the strengths of DL models in feature extraction and classification, and provided a detailed comparison of current state-of-the-art models for single-input-single-output (SISO) systems regarding accuracy and complexity. The paper also explored the application of DL-AMR in multiple-input-multiple-output (MIMO) scenarios with precoding, and discusses challenges and future research directions. The review emphasized the potential of DL-AMR in next-generation B5G/6G networks and the need to address issues related to complexity and explainability for practical deployment.

In 2024, the authors of [30] introduced VLCMnet, a novel deep learning model designed for modulation format recognition in indoor visible light communication (VLC) systems. VLCMnet integrated a temporal convolutional network with a long short-term memory (TCN-LSTM) module toward the equalization of direct channel, improving constellation diagram quality.

It also incorporated a multi-mixed attention network (MMAnet) within a CNN framework to capture detailed spatial and channel features, improving recognition accuracy. Experimental results demonstrated that VLCMnet achieves a 19.2% increase in accuracy compared to traditional CNN models, showing robustness under severe channel distortion and improving performance for high-order modulation signals. The model effectively reduced misclassification and is efficient in complex indoor environments.

The authors of [31] presented a signal modulation recognition method using deep learning, specifically SCFNet, designed for non-cooperative communication systems where transmitter parameters are unknown. SCFNet utilized a double-branch deep learning network to extract features from IQ signals and multi-channel constellations, enhancing recognition by leveraging complementary signal characteristics.

This approach improved robustness against noise and frequency offsets. Experimental results showed SCFNet achieved a recognition rate of 90% to 95%, with only a 6% accuracy decrease when frequency offsets increased from 25 kHz to 100 kHz, compared to a 15% decrease in traditional models. This demonstrated SCFNet's superior performance and robustness in challenging environments.

The study in [32] explored the use of DL, specifically CNNs, for modulation classification in communication systems, an area not extensively studied before. By converting raw modulated signals into grid-like images and employing the AlexNet model, the study presented a novel approach for classification.

The CNN-based method is compared with traditional cumulant and support vector machine (SVM) algorithms, showing comparable classification accuracy while eliminating the need for manual feature selection. Although current results are promising, the paper notes potential improvements, such as enhancing data conversion methods and

exploring advanced neural network architectures, to further boost performance.

As noted in [15], the study reviewed recent advancements in Automatic Modulation Recognition (AMR) within the context of increasingly crowded radio spectra and evolving electromagnetic environments. Emphasizing the integration of ML and DL techniques. It detailed various DL model architectures, compared their performance, and highlighted key benefits. The paper also discussed open challenges and potential future research directions, underscoring the growing significance of ML and DL in enhancing spectrum efficiency and service quality in modern communication systems.

The study in [33] presented a novel CNN-based framework for AMR of radio signals, leveraging spectrogram images derived from the short-time discrete Fourier transform. This approach, called SCNN2, improved signal recognition accuracy by transforming 1-D radio signals into time-frequency representations and applying a Gaussian filter for noise reduction. Compared to existing methods, SCNN2 outperforms other deep learning-based techniques in recognition accuracy and showed competitive results in terms of computational complexity, requiring more memory but fewer learned parameters. Overall, the SCNN2 framework demonstrated superior performance in distinguishing between modulation types while maintaining efficient training and processing capabilities.

In [34], The authors investigated the optimal DL architecture for automatic modulation identification in wireless signal recognition. By analyzing various convolutional neural network (CNN) structures, the study found that deeper networks are less suitable due to their characteristics, suggesting a preference for shallower architectures. The use of transfer learning enhanced training stability and performance. Additionally, incorporating a denoising autoencoder for data preprocessing improved recognition accuracy by mitigating noise interference. The findings highlighted the importance of adapting deep learning methods to signal recognition tasks and proposed future research directions for optimizing network design and leveraging autoencoders.

The authors of [35] developed a CNN-based modulation classification algorithm that addressed the challenge of noisy channels distorting constellation diagrams. By applying the Radon Transform (RT) to these diagrams, the study enhanced pattern representation, leading to improved classification accuracy, especially at low SNRs. The algorithm used pretrained networks such as VGG-16, AlexNet, and VGG-19 for recognition and demonstrated superior performance compared to other methods under varying channel conditions. The paper suggested exploring additional transforms like Gabor and Speeded-Up Robust Features (SURF) to further improve accuracy.

The authors of [36] paper focused on developing and evaluating two CNN models for AMR in wireless communication systems. The models were applied to two distinct datasets: RadioML2016.10a, containing 11 modulation classes, and an image-based dataset with 8 digital modulation classes. The models were fine-tuned to achieve high accuracy, with the first CNN attaining 53.65% accuracy and the second 94.39%.

III. IoUT APPLICATIONS

The Internet of Underwater Things (IoUT) is a groundbreaking technology that significantly enhances the ability to monitor, explore, and manage underwater environments. One of its primary applications is environmental monitoring, where IoUT enables the continuous tracking of water quality, temperature, pH levels, and the health of marine ecosystems. This real-time data is crucial for studying climate change, detecting pollution, and preserving biodiversity, offering invaluable insights for researchers and conservationists [37], [38], [39], [40], [41]. In underwater exploration, IoUT is revolutionizing the way we study the deep sea. Equipped with networks of sensors and autonomous underwater vehicles (AUVs), IoUT systems can map the ocean floor, discover new marine species, and investigate underwater geological formations.

These capabilities are essential for advancing our understanding of the ocean's vast and largely unexplored depths [42], [43], [44]. Disaster prevention is another critical application of IoUT. By deploying sensors that monitor seismic activity, tsunamis, and underwater volcanic eruptions, IoUT systems can provide early warnings, helping to mitigate the impact of natural disasters on coastal communities and marine infrastructure [45], [46], [47]. In the military domain, IoUT plays a pivotal role in enhancing underwater surveillance, mine detection, and secure communication among submarines and other naval assets.

It supports operations in anti-submarine warfare, port security, and the protection of underwater assets such as pipelines and communication cables [48], [49], [50]. Beyond these core applications, IoUT is also finding innovative uses in sports analysis, where it can track underwater movements in swimming or diving, providing detailed data for performance optimization [51]. In navigation assistance, IoUT helps guide submarines and other underwater vehicles through complex environments, improving safety and efficiency [52].

Location applications are another emerging area, where IoUT enables precise tracking of underwater assets, such as remotely operated vehicles (ROVs) or underwater drones, and aids in the management of marine operations [53]. Overall, IoUT applications are transforming how we interact with the underwater world, making significant contributions to environmental protection, scientific research, disaster resilience, military strategy, and industrial efficiency.

In conclusion, the IoUT offers transformative benefits across multiple domains, from environmental monitoring and underwater exploration to disaster prevention and military operations. Its ability to provide real-time data and enhanced connectivity in underwater environments not only advances scientific research and conservation efforts, but also improves disaster resilience and operational efficiency in industries such as defense and navigation. As IoUT

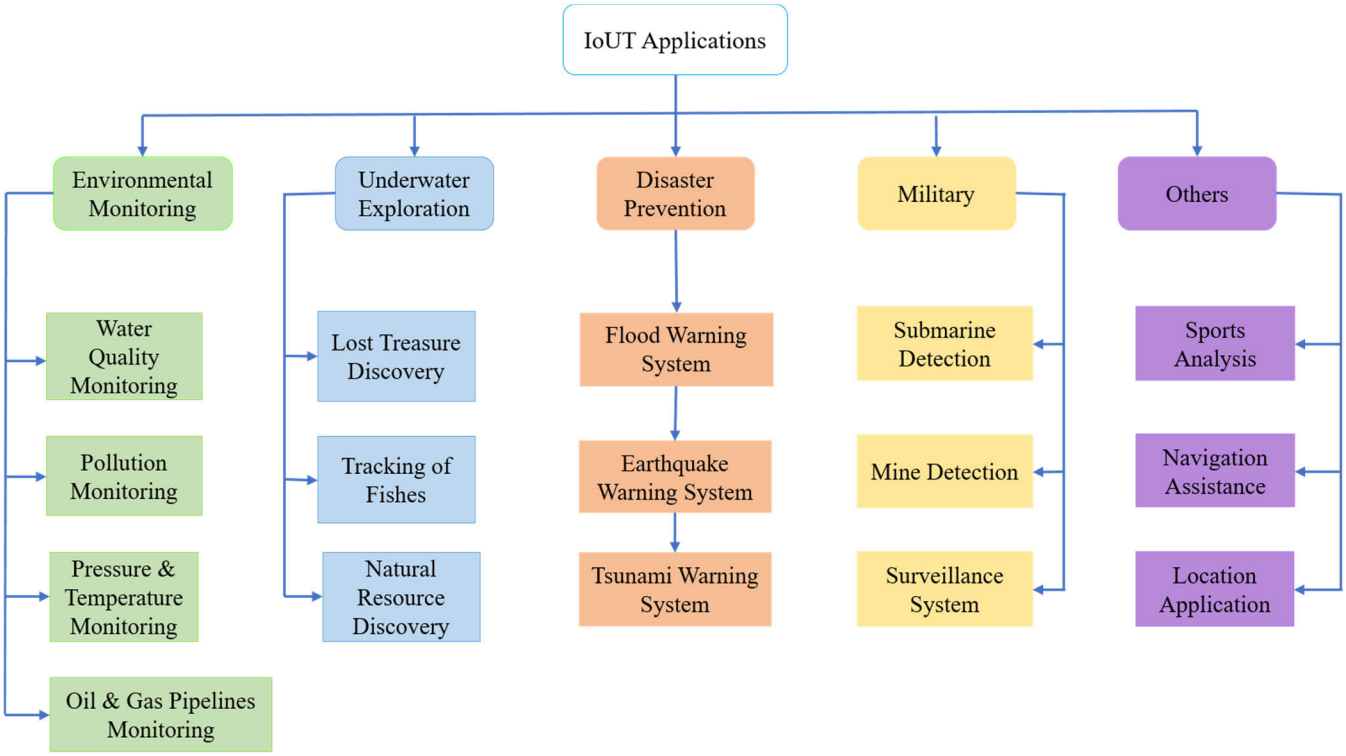

FIGURE 1. IoUT applications.

applications continue to evolve, they will play a critical role in safeguarding marine ecosystems, enhancing security, and driving innovation in underwater technology. Figure 1 illustrates the various applications of IoUT.

IV. THE PROPOSED METHODOLOGY

The proposed methodology including an underwater optical wireless communication (UOWC) system for IoUT applications. Additionally, the proposed work uses deep learning, specifically CNNs, to improve modulation recognition in underwater optical wireless systems. It involves preprocessing data, training the CNN to classify 64-QAM and 32-PSK modulations, and evaluating performance metrics to ensure accurate recognition under different underwater conditions.

A. THE PROPOSED UOWC SYSTEM

The system for this study focuses on the application of DL techniques to enhance modulation recognition in optical wireless communication systems, specifically for IoUT applications. The model incorporates a deep CNN designed to recognize modulation schemes such as 64-QAM and 32-PSK, which are crucial for high-speed data transmission in underwater environments. The optical communication channel is characterized by significant attenuation and scattering, necessitating robust signal processing methods. The CNN model processes received signal data, represented as constellation diagrams, to automatically learn and extract features pertinent to modulation recognition. The proposed system is designed to operate under varying underwater conditions, including different levels of SNR and channel impairments, ensuring accurate classification despite the challenging underwater environment. The integration of deep learning into this system model represents a significant advancement in IoUT applications, offering improved reliability and efficiency in underwater communication. A typical UOWC system comprises a sink node placed at the water's surface, which could be a buoy, surface ship, or surface autonomous vehicle (SAV), and another node located on the ocean floor. This underwater node could be a submari'e, sea diver, sensor, autonomous underwater vehicle (AUV), or unmanned underwater vehicle (UUV) responsible for gathering information and transmitting data to the sink node. The sink node, in turn, relays the data to a remote monitoring center on the shore, where the information is collected, analyzed, and processed.

Figure 2 illustrates the architecture of UOWC system model. The proposed UOWC system presents several advantages over traditional acoustic and RF systems in underwater environments. The UOWC provides high-speed data transmission with low latency, making it optimum for real-time applications. This system also experiences less signal attenuation compared to RF signals, which are heavily absorbed by water, especially at greater depths. Unlike acoustic systems, which suffer from low data rates and significant signal

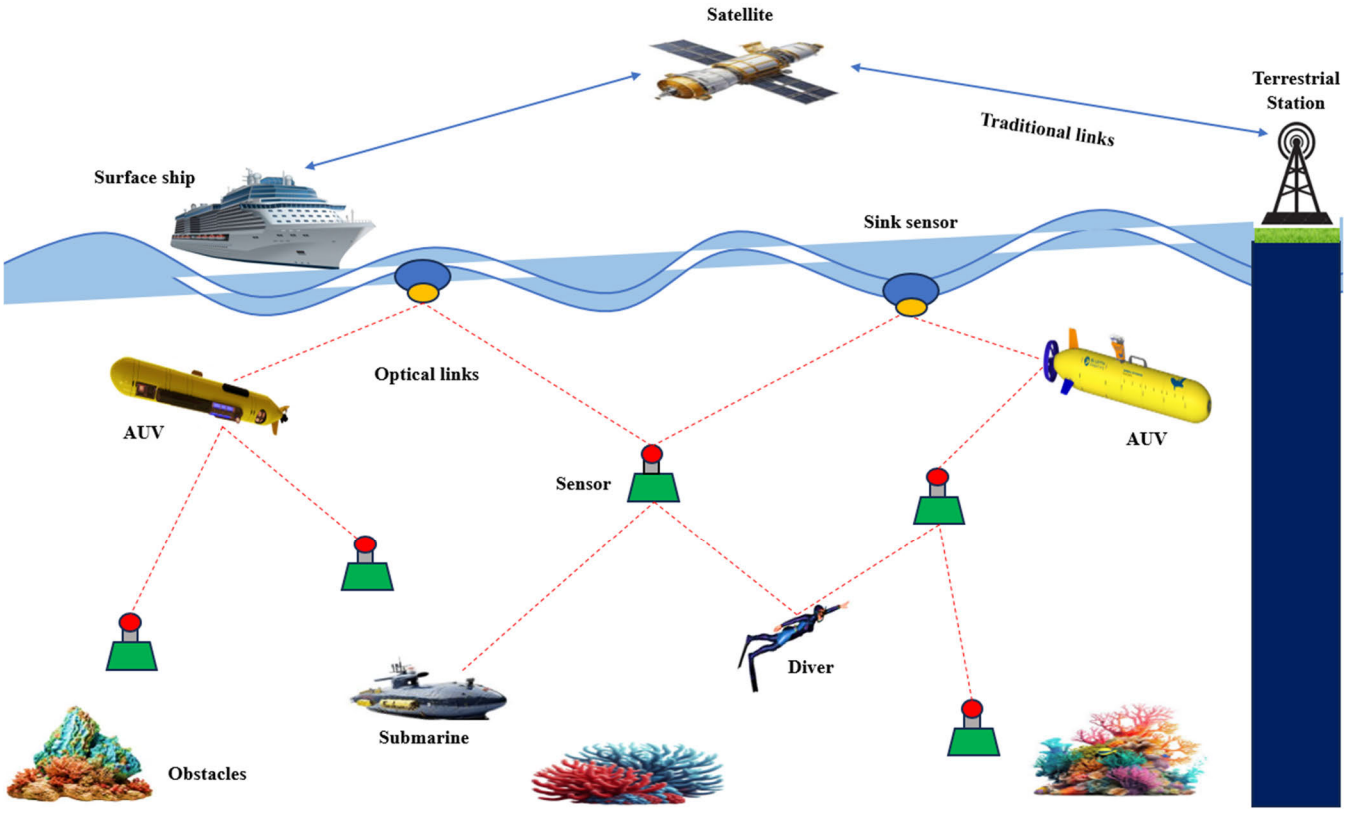

FIGURE 2. The UOWC system architecture.

delay. Furthermore, the UOWC enables higher bandwidth and supports faster, more reliable communication, making it convienent for high-data-rate fields for instance complex sensor networks and video streaming. These benefits make the UOWC a promising solution for enhancing underwater communication efficiency and performance.

B. THE BLOCK DIAGRAM OF THE UOWC SYSTEM

The overall flow of the system can be summarized as: Optical Transmitter → Optical Channel → Optical Receiver → Feature Extraction → Deep Learning Model → Output. This block diagram outlines the conceptual structure of the system, detailing how the optical signal is transmitted, processed, and analyzed to achieve deep learning (DL)-based modulation recognition in an UOWC system. Figure 3 illustrates the conceptual structure of the block diagram of the proposed UOWC system.

The system can be structured into several key components. The Optical Transmitter is the first component, where a signal source generates the baseband signal, modulated using either 64-QAM or 32-PSK. This modulated signal is then converted into an optical signal by the optical source, typically a laser diode or LED, driven by a driver circuit. The signal then passes through the Optical Channel, which represents the underwater environment. This channel includes factors like water medium that affects signal propagation, attenuation, and scattering due to water absorption. The channel also models various noise sources, such as thermal noise, shot noise, and interference from ambient light, which can degrade the signal quality. Upon reaching the Optical Receiver, the optical signal is converted back into an electrical signal by a photodetector. This weak signal is then amplified and digitized using an analog-to-digital converter (ADC) for further processing. Next, in the Feature Extraction stage, a signal processing block extracts essential features from the received signal. These features may include phase, amplitude, frequency, and constellation points, which are critical for identifying the modulation scheme. The extracted features are then fed into a DL Model, where pre-processing normalizes the data and prepares it for input into the neural network. This network, typically a CNN or another DL architecture, is trained to recognize the modulation type, whether it is 64-QAM or 32-PSK, based on the extracted features. The model then classifies and outputs the predicted modulation type. Finally, the Output block represents the system's conclusion, determining the modulation scheme used—either 64-QAM or 32-PSK. Optionally, performance metrics such as recognition accuracy and bit error rate (BER) can be evaluated to assess the effectiveness of the system.

In summary, the system processes underwater optical signals modulated using 64-QAM or 32-PSK, transmitting

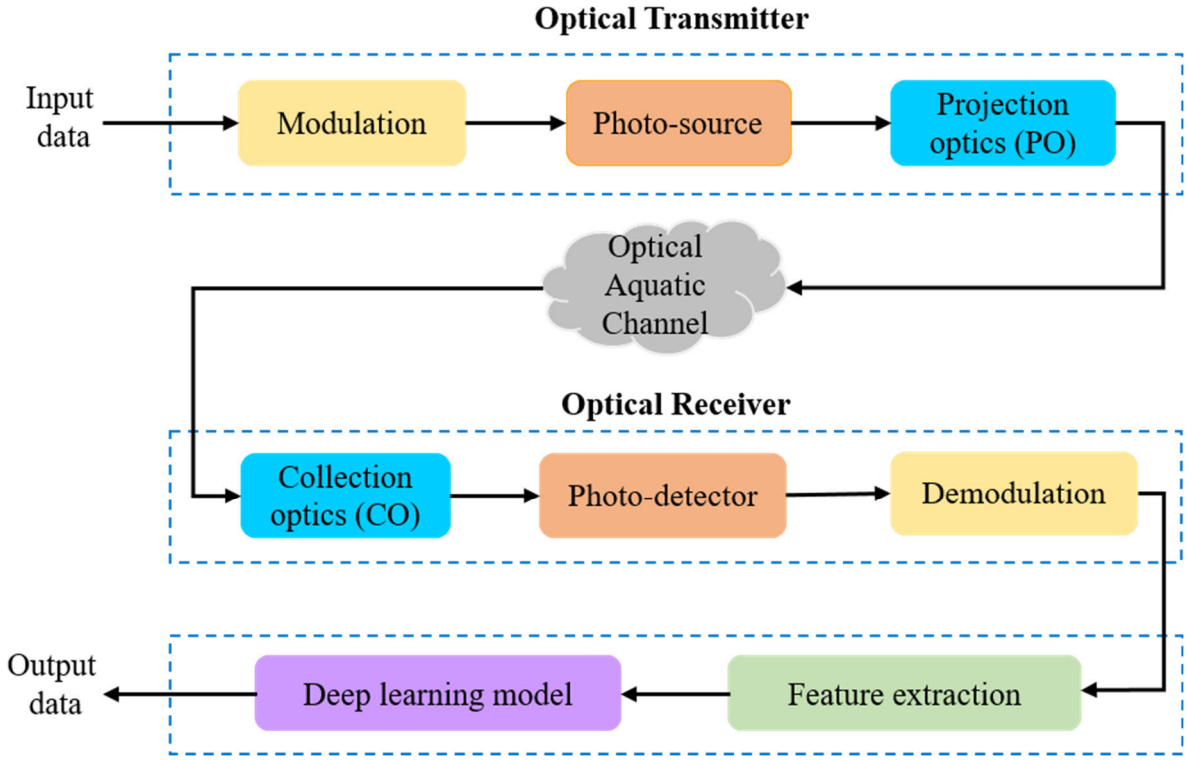

FIGURE 3. The block diagram of the proposed UOWC system.

them through an optical channel impacted by noise and water absorption. After feature extraction, a CNN deep learning model classifies the modulation type based on the received signal, with performance metrics like accuracy and BER assessing the system's effectiveness.

1) MODULATION TECHNIQUES

Quadrature Amplitude Modulation (QAM) transmits data by varying both the amplitude and phase of the carrier signal. For 64-QAM, the modulated signal can be expressed as:

$$S_{64QAM}(t) = Re\left\{(I_k + jQ_k)\, e^{i2\pi f_c t}\right\} \tag{1}$$

where I_k and Q_k represent the in-phase and quadrature components, respectively, chosen from a constellation of 64 points, f_c is the carrier frequency, and t represents time. The constellation points are defined as: $I_k, Q_k \in \{\pm\frac{2m-1}{\sqrt{42}}, m = 1, 2, 3, 4\}$ with a normalized average power to ensure that the transmitted power remains constant. Phase Shift Keying (PSK) modulates the phase of the carrier signal. For 32-PSK, the modulated signal can be written as:

$$S_{32PSK}(t) = \cos(2\pi f_c t + \theta_k) \tag{2}$$

where $(\theta_k = \frac{2\pi k}{32}, k = 0, 1, \ldots\ldots, 31)$ represents the phase of the signal, f_c is the carrier frequency. The constellation points for 32-PSK are uniformly spaced on a circle in the complex plane.

2) CHANNEL MODEL

The optical wireless communication channel in underwater environments can be modeled by considering the effects of absorption, scattering, and turbulence. The received optical power P_r at a distance d can be defined as:

$$P_r(d) = P_t.\eta_t.\eta_r.\frac{A_r}{d^2}.e^{-\gamma d}.T \tag{3}$$

where P_t is the transmitted power, η_t and η_r are the efficiencies of the transmitter and receiver, Ar is the receiver aperture area, γ is the total attenuation coefficient, which accounts for absorption and scattering, and $T(\Theta)$ is the beam spread function, accounting for the angle of incidence Θ.

$$\gamma(\Lambda) = \alpha(\lambda) + \beta(\lambda) \tag{4}$$

where $\alpha(\lambda)$ and $\beta(\lambda)$ are the absorption and scattering coefficients of the light as a function of wavelength.

Blue and green wavelengths are favored in underwater optical wireless communication (UOWC) due to their lower attenuation values compared to other wavelengths. In clear ocean waters, blue light (around 450 nm) undergoes minimal absorption and scattering, making it ideal for long-distance communication. Green light (around 520 nm) is more effective in coastal and turbid waters, where it penetrates better than other wavelengths. These wavelengths significantly reduce signal loss, providing a substantial advantage over red or infrared wavelengths, which are rapidly absorbed in water, limiting their effectiveness for underwater communication.

Figure 4 presents the light absorption coefficient as a function of wavelength in pure seawater.

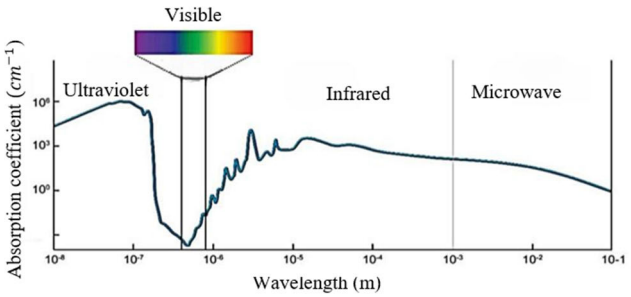

FIGURE 4. The absorption coefficient of the light as a function of wavelength in pure seawater [54].

Tables 1 and 2 present the absorption and scattering coefficients for different types of water at wavelengths of 450 nm and 520 nm, respectively. These coefficients are critical in UWOC systems because they directly affect the attenuation of light as it propagates through water. The absorption coefficient $\alpha\lambda$) measures how much light is absorbed by the water molecules and particles. Higher absorption values indicate that more light is absorbed, reducing the amount of optical power that can be transmitted over longer distances. For example, in turbid harbor waters, where $\alpha\lambda$) is significantly higher than in pure sea water, the light signal is absorbed more quickly, limiting the effective communication range. Based on the equations of absorption and scattering of the light in [55], The absorption, scattering, and extinction coefficients are determined for various types of water for two sources, LED-PS and LD-PS at operational wavelengths 450 nm (blue) and 520 nm (green). These calculations are presented in Tables 1 and 2.

TABLE 1. Absorption, Scattering, and extinction coefficients for different types of at wavelenght = 450 nm [54].

Types of Water	Absorption Coefficient $\alpha(\lambda)$ (m^{-1})	Scattering Coefficient $\beta(\lambda)$ (m^{-1})	Extinction Coefficient $\gamma(\lambda)$ (m^{-1})
Pure Sea	0.03899	0.0009495	**0.0399395**
Clear Ocean	0.07888	0.01281	**0.09169**
Costal Ocean	0.2967	0.1041	0.4008
Turbid Harbor	2.276	0.5499	2.8259

The scattering coefficient β (λ) refers to the deflection of light caused by particles and turbulence in the water. The scattering coefficient affects the beam's directionality and can cause loss of signal strength, especially in environments with high particulate matter, like coastal or turbid waters. Scattering also leads to multipath interference, which impacts

TABLE 2. Absorption, Scattering, and extinction coefficients for different types of at wavelenght = 520 nm [54].

Types of Water	Absorption Coefficient $\alpha(\lambda)$ (m^{-1})	Scattering Coefficient $\beta(\lambda)$ (m^{-1})	Extinction Coefficient $\gamma(\lambda)$ (m^{-1})
Pure Sea	0.04418	0.0009092	0.0450892
Clear Ocean	0.08642	0.01226	0.09868
Costal Ocean	0.2179	0.09966	**0.31756**
Turbid Harbor	1.112	0.5266	**1.6386**

the quality of the received signal. The extinction Coefficient $\gamma\lambda$) is the sum of the absorption and scattering coefficients ($\gamma\lambda$) = $\alpha\lambda$) + $\beta\lambda$)), representing the total attenuation of the light beam in the water. The higher the extinction coefficient, the greater the attenuation, and therefore, the more challenging it becomes to establish reliable optical communication.

These coefficients vary significantly across different water types, with turbid harbor waters exhibiting the highest levels of absorption and scattering. This variation highlights the need to carefully select wavelengths and system parameters based on the specific water environment. For instance, shorter wavelengths like 450 nm may be more suitable for clearer water types due to lower absorption, while in more turbid environments, the choice of wavelength and beam divergence must be optimized to minimize attenuation and maintain signal integrity so 520 nm is suitable to use in coastal and turbid waters. By analyzing these coefficients, we can model the underwater optical channel more accurately and tailor the system for optimal performance under various water conditions [56], [57].

From the results calculated from Tables 1 and 2, we can conclude that the blue color wavelength (λ = 450 nm) is appropriate for pure seawater and clear ocean water because of the minimum extinction coefficient values in those two types of water compared with the green color. On the other hand, the green color wavelength (λ = 520 nm) is convenient for water whether form a coastal ocean or turbid harbor [56], [57].

3) TURBULENCE MODEL

The Log-Normal fading distribution model is widely used to describe the statistical behavior of the signal amplitude in UWOCs, particularly under weak turbulence conditions. In such environments, turbulence is caused by small-scale fluctuations in the refractive index of water, which can be influenced by salinity, temperature, and pressure. These factors affect the propagation of optical signals in water,

leading to variations in signal strength over time, often modeled as Log-Normal fading.

Regarding the Log-Normal fading model, it assumes that the logarithm of the received signal intensity follows a normal (Gaussian) distribution. The probability density function (PDF) for the received signal intensity I under Log-Normal fading is given by:

$$f_I(I) = \frac{1}{I\sigma\sqrt{2\pi}} exp\left(-\frac{(\ln(I)-\mu)^2}{2\sigma^2}\right) \tag{5}$$

where I is the received signal intensity, μ is the mean of the logarithm of the received intensity $ln(I)$, σ is the standard deviation of $ln(I)$, representing the severity of fading, and $ln(I)$ follows a normal distribution with mean μ and variance σ^2. In UWOCs, fluctuations in the refractive index, caused by environmental factors such as salinity, temperature, and pressure, lead to variations in the received signal intensity. These variations are captured by the standard deviation σ, which increases with the strength of the turbulence.

Regarding effects of environmental factors on Log-Normal fading in UWOCs, in underwater environments, salinity, temperature, and pressure affect the refractive index of water, which in turn influences the optical signal's propagation characteristics, leading to turbulence and fading. Let's discuss how each factor relates to the Log-Normal fading distribution in UWOCs. **Salinity** refers to the concentration of dissolved salts in water. As salinity increases, the refractive index of water changes, affecting how light propagates through the medium. The relationship between salinity and refractive index can be expressed as:

$$n = n_o + k_s S \tag{6}$$

where n is the refractive index of water, n_o is the refractive index of pure water, K_s is a proportionality constant that depends on the wavelength of the light, and S is the salinity of the water. Increased salinity can cause scattering and absorption of light, leading to more severe fading. The parameter σ^2 in the Log-Normal fading model increases as salinity-induced turbulence grows stronger, thereby causing larger signal fluctuations and a higher probability of deep fades. **Temperature** variations also cause changes in the refractive index, due to thermal expansion and contraction of water. The relationship between temperature and refractive index is given by:

$$n(T) = n_o - k_T (T - T_o) \tag{7}$$

where T is the water temperature, n_o is the refractive index at a reference temperature T_0, and k_T is a temperature-dependent constant. As the temperature fluctuates, the refractive index varies, creating turbulence in the water that affects signal propagation. Higher temperature gradients lead to greater variations in signal intensity, increasing the standard deviation σ in the Log-Normal model. This causes more pronounced fading, resulting in signal attenuation and fluctuations in SNR. **Pressure** increases with water depth, and changes in pressure can affect water density, which in turn influences the refractive index. The relationship between pressure and the refractive index can be expressed as:

$$n(P) = n_o + k_P P \tag{8}$$

where P is the water pressure, n_o is the refractive index at a reference pressure, and k_P is a pressure-dependent constant. As pressure increases with depth, variations in the refractive index can cause scattering and refraction of light, leading to signal fading. In deep-water environments, the pressure-induced turbulence results in higher values of σ, increasing the severity of fading and thus degrading the communication performance. The Log-Normal fading distribution model is crucial for understanding signal propagation in UWOCs, especially under the influence of environmental factors such as salinity, temperature, and pressure. These factors affect the refractive index of water, leading to turbulence and signal fading. As salinity, temperature, and pressure increase, the severity of fading increases (represented by a higher standard deviation σ, leading to degradation in SNR, BER, and channel capacity. Addressing these challenges requires the implementation of adaptive techniques and robust communication strategies.

4) SIGNAL-TO-NOISE RATIO (SNR)

The SNR at the receiver is calculated in Eq. (9). Where P_r is the received signal power, N_0 is the noise power spectral density, B is the bandwidth of the system. For optical wireless communication systems, noise sources include background shot noise, thermal noise, and signal shot noise, leading to the total noise power N_0.

$$SNR = \frac{P_r}{N_o B} \tag{9}$$

The dataset was generated using a range of SNR values from 0 dB to 30 dB in steps of 5 dB, covering both challenging and favorable underwater conditions. The model was trained and tested under these different SNR conditions to evaluate its performance in realistic underwater optical communication scenarios.

The dataset incorporates several noise types typically encountered in UWOCs, including:

(i) Background shot noise from ambient light interference. (ii) Thermal noise due to the receiver's electronics. (iii) Signal shot noise, which arises from the randomness in the optical signal.

Eq. (10) shows the total noise power spectral density No.

$$N_o = N_{shot} + N_{thermal} + N_{signal-shot} \tag{10}$$

where N_{shot} is the background shot noise power spectral density (W/Hz), $N_{thermal}$ is the thermal noise power spectral density (W/Hz), and $N_{signal-shot}$ is the signal shot noise power spectral density (W/Hz). Eq. (11) describes the Shot Noise (Background) N_{shot}.

$$N_{bg-shot} = 2qI_{bg}B \tag{11}$$

where $P_{bg-shot}$ is the back ground shot noise power, q is the electron charge 1.602×10^{-19} C), I_{bg} is the background current (A), and B is the bandwidth (Hz). Eq. (12) describes Thermal Noise $N_{thermal}$.

$$N_{thermal} = \frac{4KTB}{R_L} \tag{12}$$

where $N_{thermal}$ is the thermal noise power, K is the Boltzmann constan (1.38×10^{-23} J/K), T is the absolute temperature (K), and R_L is the load resistance (Ω). Eq. (13) describes Signal Shot Noise $N_{signal-shot}$.

$$N_{signal-shot} = 2qI_{signal}B \tag{13}$$

where is the signal shot noise power $N_{signal-shot}$, I is the average signal current (A).

These noise models were included to ensure that the dataset reflects real-world underwater conditions, allowing the CNN model to learn and classify modulation schemes accurately in the presence of noise. Despite the presence of various noise types and varying SNR levels, the CNN model achieved 100% accuracy in certain scenarios, particularly under higher SNR conditions ($\geq$20 dB). This high accuracy is attributed to the model's ability to effectively capture the features of different modulation schemes, even in the presence of moderate noise. The 100% accuracy reflects the robustness of the model under ideal or less challenging conditions, while performance at lower SNR values still remained competitive, demonstrating its applicability across different underwater environments.

5) BIT ERROR RATE (BER)

The BER for 64-QAM and 32-PSK can be calculated using their respective probability of error expressions. The general law for M-QAM and M-PSK can be expressed in Eqs. (14) and (15). M represents the number of distinct symbols in the modulation scheme, while $Q(x)$ is the Q-function, representing the tail probability of a Gaussian distribution.

$$BER_{M-QAM} = \frac{4}{Log_2(M)} \cdot \left(1 - \frac{1}{\sqrt{M}}\right) \cdot Q\left(\sqrt{\frac{3Log_2(M)}{M-1} \cdot SNR}\right) \tag{14}$$

$$BER_{M-PSK} = \frac{1}{Log_2(M)} \cdot Q\left(\sqrt{2.SNR} \cdot Sin\left(\frac{\pi}{M}\right)\right) \tag{15}$$

In case of 64-QAM and 32-PSK Eqs. (14) and (15) can be expressed as:

$$BER_{64-QAM} = \frac{7}{12} \cdot Q\left(\sqrt{\frac{2}{7} \cdot SNR}\right) \tag{16}$$

$$BER_{32-PSK} = \frac{1}{5} \cdot Q\left(\sqrt{2.SNR} \cdot Sin\left(\frac{\pi}{32}\right)\right) \tag{17}$$

6) DEEP LEARNING-BASED MODULATION RECOGNITION

The modulation recognition is implemented using a CNN, which takes as input the received signal samples and outputs the predicted modulation type. The signal samples are represented as complex baseband equivalents in Eq. (18). Where $s(t)$ is the transmitted signal and $n(t)$ is the noise.

$$r(t) = s(t) + n(t) \tag{18}$$

The CNN is trained to minimize the cross-entropy loss function:

$$L = -\sum_{i=1}^{N} y_i log\hat{y}_i \tag{19}$$

where y_i is the actual label, $\hat{y}_i$ is the predicted output probability for class I, and N is the number of classes (e.g., 64-QAM and 32-PSK).

7) DATASET GENERATION AND SIMULATION

We generated a dataset of 64-QAM and 32-PSK modulated signals using a simulated underwater optical communication system. The simulation included varying levels of absorption, scattering, and turbulence to replicate different underwater conditions. Absorption and scattering are modeled based on empirical data for various water types, including coastal, clear, and turbid water. Turbulence is simulated using a stochastic model to account for random variations in the refractive index of water. Figure 5 shows the constellation diagrams as two samples dataset: 64 QAM and 32 PSK.

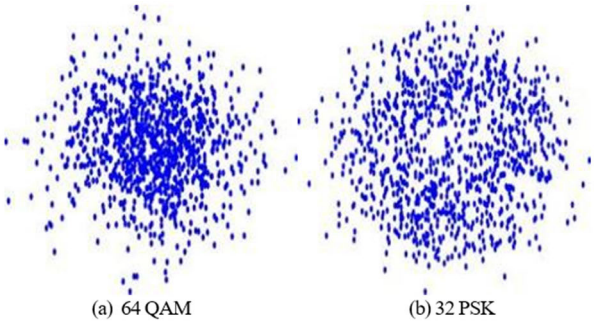

FIGURE 5. Two samples of the dataset: (a) 64 QAM, (b) 32 PSK.

To prepare the data for CNN training, we applied three preprocessing steps: noise Reduction, normalization, and segmentation. Noise reduction using a low pass filter (LPF) to reject a high-frequency noise from the signal. Normalization of signal amplitude is used to ensure consistency across samples, while segmentation is applied to divide signals into smaller segments, enabling the CNN to process and learn from localized features. The utilized datasets are public available in the Kaggle repository [58] https://www.kaggle.com/datasets/drsaeedmohsen/radio-modulation-types-dataset. The datasets are seperated into learning (80%) and evaluation (20%) sets. Training involved adjusting the model parameters to minimize the classification error. Three data augmentation approaches are applied for the used dataset, such as rotation, width and height shifts. Randomly, each image is rotated by 20°, with width and height shifted by up to 0.2 in both dimensions.

In the study on deep learning-based modulation recognition for OWCs in IoUT applications, several key parameters are defined. The modulation schemes under investigation include 64-QAM and 32-PSK, which represent the types of signal modulation utilized. The optical wavelength for the transmitted signals is set to 450 nm (blue) and 520 nm (green), addressing different underwater environments.

The optical sources used in the simulation are either laser diodes (LD) or light-emitting diodes (LED), with transmission power ranging from 10 mW to 100 mW. Receiver sensitivity, which determines the minimum detectable power level at the receiver, is specified between −50 dBm and −70 dBm. The water types considered in the simulation include clear ocean, coastal, and turbid waters, each affecting signal propagation differently.

For photodetection, avalanche photodiodes (APD) and PIN diodes are employed. The data transmission rate varies from 1 Mbps to 10 Gbps, and the sampling rate of the received signal is between 10 GHz and 100 GHz. The channel model used to simulate the underwater optical channel includes Log-Normal and Generalized Gamma distributions. Finally, performance metrics for evaluating the system include accuracy, bit error rate (BER), and SNR.

8) THE PROPOSED FRAMEWORK FOR THE DEVELOPED CNN MODEL

Figure 6 shows the proposed framework for the CNN Model. It includes 626 modulation images as a dataset that is initially preprocessed. Moreover, the data is divided into x_train with its label y_train and x_test with its label y_test. The training data is reshaped to match the dimensions of the convolutional layers, then the CNN layers are architected, then the model is compiled based on the optimizer, cost function, and accuracy metric. So, it is very essential to set optimum settings to minimize the error of the CNN.

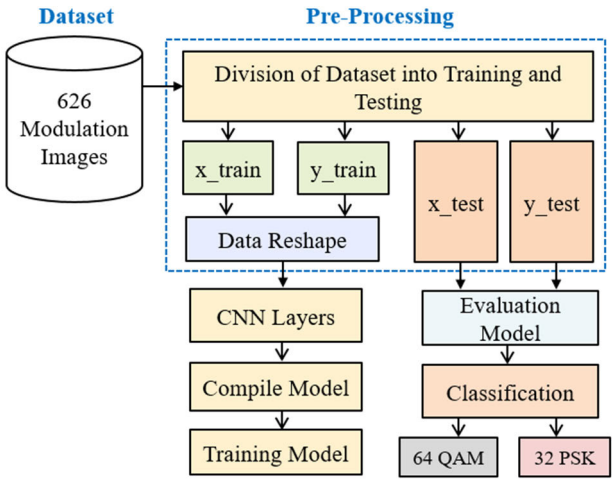

FIGURE 6. The proposed framework for the steps of CNN implementation.

After that, the model is learned/trained from the features of training images dataset. Then, the CNN model is evaluated using x_test and y_test, hence the validation of fitting for the CNN based on testing and training datasets. Finally, the classification is implemented via a predict command using the x_test as new unseen dataset with respect to the trained model. The prediction phase provides a probability of classes whether 64 QAM or 32 PSK. Furthermore, the predictive CNN model can compare a true label to a predicted class via an evaluation metric e.g. confusion matrix.

9) THE PROPOSED CNN MODEL ARCHITECTURE

In this research, a CNN is utilized to identify the modulation types. The CNN architecture is particularly effective to capture spatial features from data. Figure 7 depicts the CNN architecture consists of twelve layers: three convolutional layers, three max-pooling layers, two dropout layers, one flattening layer, two dense layers, and an output layer. Adam optimizer is used to minimize the error of CNN and a cross-entropy loss function is applied.

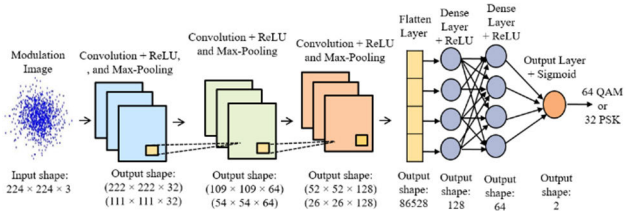

FIGURE 7. The proposed CNN model architecture.

The modulation images input has a resolution of 224 × 224 pixels. Initially, a 2D convolutional layer (conv2D) is applied to each input image separately using a ReLU activation function to learn spatial features. This layer extracts local features from the signal, such as amplitude variations and phase shifts. This layer contains 32 filters with a 3 × 3 kernel. To mitigate the risk of overfitting, a dropout layer is introduced next.

Following this, a max-pooling layer (MPL) is employed to reduce the complexity of the conv2D by downsampling it (to reduce the dimensionality of the data. The MPL uses a 2 × 2 matrix as its pool size. Subsequently, another conv2D layer is introduced, this time with 64 filters and a 3 × 3 kernel, paired with a ReLU function to identify higher-level features that the initial conv2D layer may have missed.

Next, another MPL with a 2 × 2 pool size is used, followed by a conv2D layer with 128 filters and a 3 × 3 kernel. This is succeeded by another MPL and a flattening layer, which transforms the data into a one-dimensional format. Then, a dense layer with 64 neurons and a ReLU is added. This is followed by a dropout layer with a 50% drop rate and another dense layer.

Finally, the output layer is connected to a sigmoid function to activate the outcome to two classes, which make the final classification decision. The sigmoid provides a probability distribution over the possible modulation schemes (64-QAM and 32-PSK). The entropy loss is applied to calculate the error among predicted and actual values, with the Adam

optimization function employed for training. The CNN model is trained for 50 epochs with a batch size of 32, and the total parameters that is trained in the CNN is 11,177,346. The hyperparameters of the CNN model are optimized via the GridSearchCV method, which automatically determines the best hyperparameter values to enhance the model's performance. Table 3 provides a sequence of the CNN layers.

TABLE 3. The layers of the CNN.

Layer	Type	Kernel Size	Output Shape
1	Conv2D	3 × 3	222 × 222 × 32
2	Dropout	-	222 × 222 ×32
3	Max-Pooling2D	2 × 2	111 × 111 × 32
4	Conv2D	3 × 3	109 × 109 × 64
5	Max-Pooling2D	2 × 2	54 × 54 × 64
6	Conv2D	3 × 3	52 × 52 × 128
7	Max-Pooling2D	2 × 2	26 × 26 × 128
8	Flatten	-	86528
9	Dense	-	128
10	Dropout	-	128
11	Dense	-	64
12	Output	-	2

Total trainable parameters: 11, 177, 346

10) PERFORMANCE METRICS

We evaluated the model using the following metrics. Accuracy is the percentage of correctly classified samples. Precision and Recall are measures of the model's performance for each modulation scheme, while F1-score is a combined metric that balances precision and recall. The efficiency of the modulation recognition system is measured utilizing the four metrics: accuracy, precision, recall, and F1-score, defined as:

$$Accuracy = \frac{TP + TN}{TP + FP + TN + FN} \tag{20}$$

$$Precision = \frac{TP}{TP + FP} \tag{21}$$

$$Recall = \frac{TP}{TP + FN} \tag{22}$$

$$F1 - score = 2 \times \frac{Precision \times Recall}{Precision + Recall} \tag{23}$$

where the statistics "*TP*, *TN*, *FP*, and *FN*" are true and false whether positives or negatives.

V. EXPERIMENTAL RESULTS

The CNN model was experimentally developed using the Python programming language within a Spyder program. The implementation was performed on a laptop equipped with an Intel Core i7 processor, operating at 3.1 GHz, with six CPUs, 16 GB of RAM, and Microsoft Windows 10 as the operating system.

Figure 8 presents the accuracy curves for both testing and training of the CNN. The orange curve represents the training accuracy, which began 61.6% and improved steadily with an increase in the training epochs, reaching 100% after 50 epochs. The green curve illustrates the testing accuracy, which started at 79.37% and also reached 100% at 50 epochs.

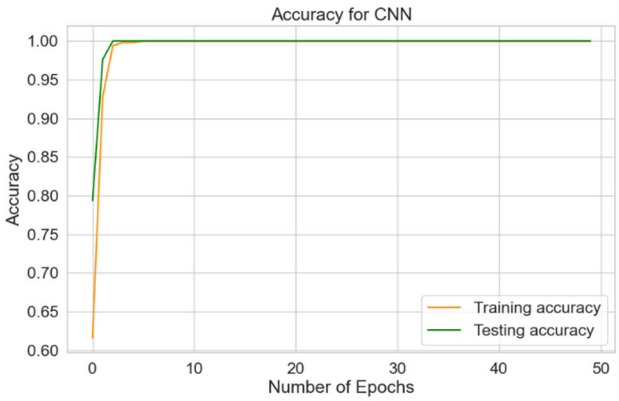

FIGURE 8. Accuracy curves for CNN.

Figure 9 depicts the loss rate curves for the CNN model using both training and testing datasets. The loss gradually decreased during training, with the test loss starting at 0.4222 and eventually reducing to 1.82×10^{-6}. For the training dataset, the loss rate started at 7.8032 and dropped to 9.8×10^{-6} after 50 epochs.

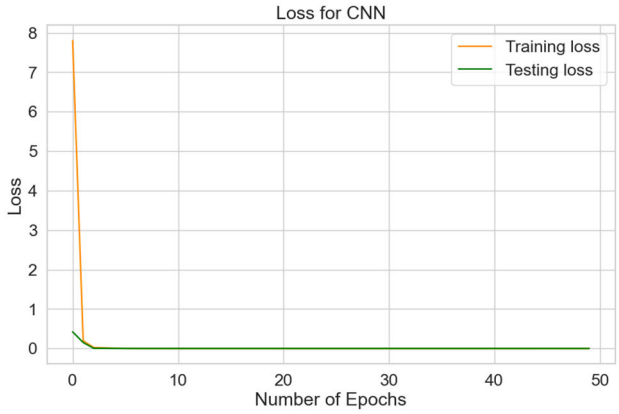

FIGURE 9. Loss curves for CNN.

Figure 10 displays the confusion matrix generated by the CNN, which illustrates the model's ability to differentiate between 2 classes utilizing the data of testing. The matrix compares the actual label output with the predicted outcome, with the dark purple squares representing correct classifications. The confusion matrix correctly identifies 62 true positives for 64QAM and 64 true positives for 32PSK, while the values outside these blocks indicate any misclassifications.

Figure 11 illustrates the normalized confusion matrix (NCM) for the CNN model, showing a perfect recognition

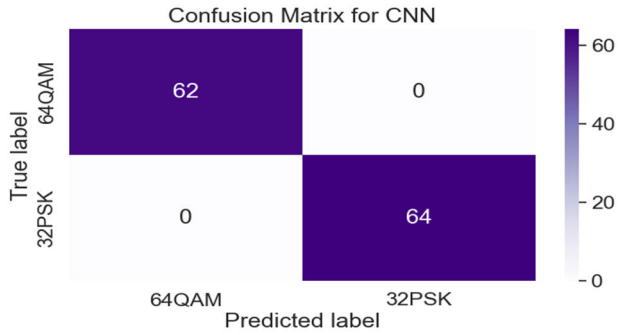

FIGURE 10. The confusion matrix for CNN.

accuracy of 1.0 (100%) for both the 64QAM and 32PSK classes, with no errors in distinguishing between them. This matrix highlights the model's ability to minimize classification errors.

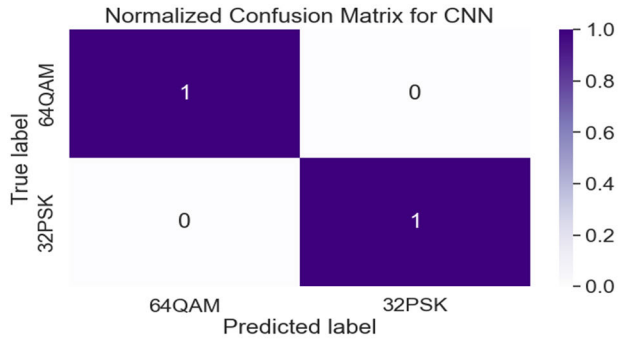

FIGURE 11. The NCM for CNN.

Table 4 details the classification report for the CNN, outlining key performance metrics such as Precision, Recall, and F1 score based on the dataset used. For the 64QAM class, all metrics—Precision, Recall, and F1 score—are at 100%. Similarly, the 32PSK class also achieved 100% for these metrics. The CNN's weighted average for Precision, Recall, and F1-score is 100%. The macro-average is calculated by independently assessing each class's metrics and then averaging the results.

TABLE 4. Classification report for CNN.

Class	Precision	Recall	F1-score
64QAM	1.0000	1.0000	1.0000
32PSK	1.0000	1.0000	1.0000
Accuracy	-	-	1.0000
Macro average	1.0000	1.0000	1.0000
Weighted average	1.0000	1.0000	1.0000

Figure 12 presents histograms for the 64QAM and 32PSK images. Figures 13 and 14 depict the Precision-Recall (PR) and ROC curves, respectively, with PR curves showing precision as a function of recall.

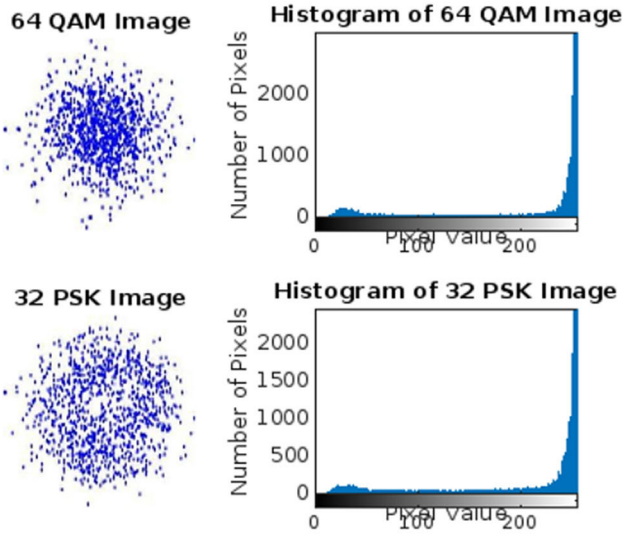

FIGURE 12. Histograms of 64 QAM and 32 PSK images.

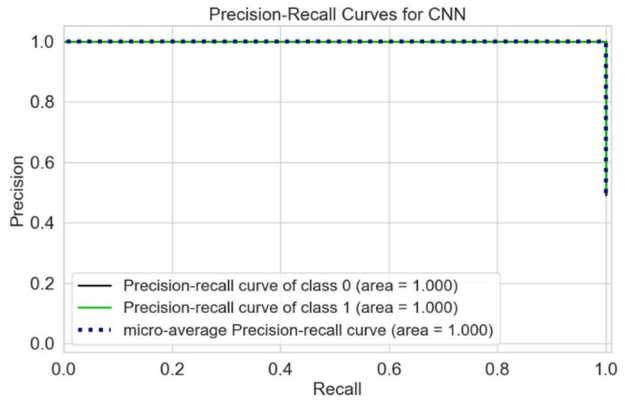

FIGURE 13. PR curves for CNN.

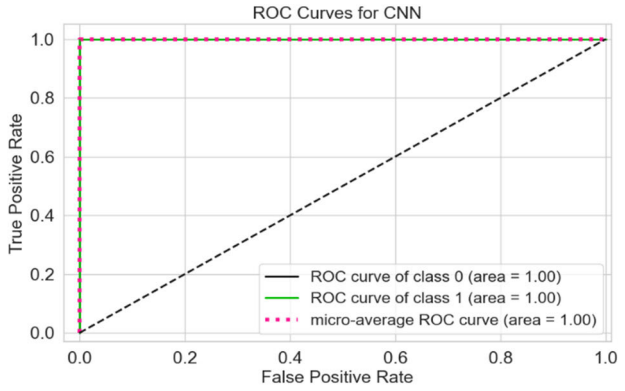

FIGURE 14. ROC curves for CNN.

Figure 13 presents the PR curves for each class, with both class 0 "64QAM" and class 1 "32PSK" achieving a perfect area of 1.000 under their respective PR curves, resulting in a micro-average PR curve area of 1.000. Figure 14 displays the ROC curves for the CNN, where the area under the curve (AUC) for both classes is 1.00, or 100%. The micro-average ROC curve also has an AUC of 1.00, indicating the model's strong performance.

TABLE 5. Comparison between the proposed work and other works.

Reference	Methodology	Key Results	Strengths	Weaknesses	Applications
[15]	Survey of AMR methods in crowded radio spectra	Reviewed various DL models and their performance, identified challenges and future research areas	Detailed examination and comparison	General review; lacks specific experimental data	Modern communication systems
[19]	Modulated signals transformed into constellation images	SqueezeNet improved modulation classification accuracy and efficiency, suitable for IoUT applications	Efficient and suitable for IoUT	Limited to specific UOWC scenarios	Underwater optical wireless communication (UOWC)
[20]	Extracted 1D phase-related features from signals for classification	Achieved over 99% classification accuracy at 0 dB, superior to 2D constellation graph-based methods	High accuracy and effectiveness	May not generalize well beyond 1D features	Automatic modulation classification (AMC)
[21]	Used higher-order cumulants and threshold algorithms for modulation classification	Achieved 88%-100% accuracy across various SNRs, outperforming existing methods	High accuracy and computational efficiency	May not perform as well in very low SNR conditions	Automatic modulation classification
[22]	Voting-based deep CNN for M-QAM and M-PSK signals	Near 100% accuracy at lower SNRs, suggests potential for future network layer enhancements	Robust performance at low SNRs	Potential for high computational cost	Wireless communication systems
[23]	Sparse convolutions with depthwise and grouped convolutions	Achieved 95.5% accuracy at +30 dB SNR, compact and efficient model	High accuracy with compact model	Limited to specific datasets and SNR conditions	Intelligent communication receivers
[24]	Grouped and asymmetric convolutional layers, flow-in-flow structure	87% accuracy at 0 dB SNR, superior to state-of-the-art models in constellation-based classification	Effective at learning radio characteristics	Performance may drop under severe fading conditions	Modulation classification
[25]	Restored missing samples in time-domain signals for AMC	Enhanced classification accuracy significantly, effective in preserving signal characteristics	Robust to missing samples and noise	Needs validation with real-world data	Automatic modulation classification
[26]	Data recovery from OOK-NRZ modulated signals through Gulf seawater	Achieved seven orders of magnitude BER reduction, improved effective channel length and SNR	Significant performance improvement	Limited to specific modulated signals and conditions	Underwater optical wireless communication (UOWC)
[27]	CNN for underwater acoustic communication modulation recognition	Effective in recognizing underwater modulation methods, needs improvement for low-SNR conditions	Effective signal recognition from raw data	Performance under low-SNR needs improvement	Underwater acoustic communication
[28]	Reviewed deep learning for AMR in 5G systems	Highlighted advantages and limitations of deep learning techniques, offered future research directions	Comprehensive review; highlights advancements	General review; lacks specific experimental results	5G wireless communication
[29]	Compared DL with traditional AMR methods	DL models excelled in accuracy and false alarm rates, explored MIMO scenarios and future research directions	Detailed comparison; future research directions	Complexity and practical deployment issues	Next-generation B5G/6G networks
[30]	TCN-LSTM and MMAnet for indoor VLC systems	19.2% accuracy increase compared to traditional CNNs, robust under severe channel distortion	Effective for high-order modulation signals	May need adaptation for other types of communication	Indoor visible light communication
[31]	Double-branch deep learning network for non-cooperative systems	90%-95% recognition rate, superior robustness against noise and frequency offsets	High robustness to noise and frequency offsets	Limited to specific non-cooperative scenarios	Non-cooperative communication systems

TABLE 5. *(Continued.)* **Comparison between the proposed work and other works.**

[32]	Converting raw modulated signals into images for classification	Comparable accuracy to traditional methods, eliminating manual feature selection	Novel approach with promising results	Potential for further improvements in data conversion	Communication systems modulation classification
[33]	CNN-based framework using spectrogram images	Improved recognition accuracy, competitive in computational complexity	Effective in time-frequency domain; competitive with existing methods	Requires more memory; fewer learnable parameters	Radio signal modulation recognition
[34]	Analyzed deep learning structures for modulation classification	Shallower networks preferred, transfer learning and autoencoders enhanced accuracy	Optimized architecture for signal recognition	Shallower networks preferred; challenges with deep networks	Signal recognition
[35]	Applied Radon Transform to constellation diagrams	Enhanced pattern representation and classification accuracy, especially at low SNRs	Enhanced pattern representation; strong performance	Requires exploration of additional transforms	Modulation classification in noisy channels
[36]	Two CNN models were developed for automatic modulation recognition and applied to two different datasets:	First CNN achieved 53.65% accuracy; second CNN achieved 94.39%. Areas under the ROC curves were 92% and 97%, respectively	High recognition accuracy, strong performance with ROC curves, effective hyperparameter tuning	Lower accuracy in the first CNN model (53.65%), performance differences between datasets	Automatic modulation recognition for wireless communication systems
The Proposed Work	**UOWC system with an efficient CNN to differentiate two types of modulation: 64 QAM and 32 PSK**	**The UOWC system integrated with a CNN, The system demonstrates 100% classification accuracy, and effective feature extraction from noisy underwater optical channels**	**Robust ability to recognize modulation with high accuracy, robust efficiency despite noise sources and underwater channel attenuation**	**Limited to two modulation schemes, Also, the performance might degrade under extreme underwater conditions**	**Modulation Recognition in UOWC system for IoUT, marine research, environmental monitoring, and military operations**

VI. DISCUSSION

The CNN model demonstrated robustness to variations in underwater conditions. It performed well across different levels of absorption, scattering, and turbulence, showcasing its ability to adapt to dynamic channel conditions. Traditional methods exhibited lower accuracy, particularly under challenging conditions. The CNN model's automated feature extraction and learning capabilities provided a clear advantage in handling complex modulation patterns. Table 5 shows a comparison between the proposed work and other traditional methods in the previous published works. The proposed work shows robust ability to recognize modulation with high accuracy, presents an efficient feature extraction using a CNN model, thus the work presents real-time classification capabilities for 64-QAM and 32-PSK, and the UOWC system has robust performance despite noise sources and underwater channel attenuation. So, the performance metrics like recognition accuracy highlights the system's reliability. Additionally, the system is chosen for underwater applications due to its ultra-high data transmission rates, reaching up to Gbps, minimal latency, and the use of low-cost, compact transceivers. These advantages make it ideal for high-speed data transfer over moderate distances. However, the drawbacks of this model is limited to two modulation schemes (64-QAM and 32-PSK), potentially lacking versatility for more complex modulations. Also, the performance might degrade under extreme underwater conditions, such as high scattering and severe noise. Further, there is a difficulty crossing the water/air boundary, high absorption, scattering, and limited range, can be addressed by optimizing the system design. This includes using wavelength selection tailored to specific water types, employing advanced beam-forming techniques.

The proposed UOWC system can be utilized for applications, for instance marine research, environmental monitoring, military operations, and IoUT applications where robust and efficient optical communication is needed. Also, the system used for high-speed data transmission and reliable modulation recognition in challenging underwater environments.

For the CNN, setting the batch size (BS) and training epochs to 32 and 50, respectively, using a softmax activation function for the output layer with pool size and kernel of the max-pooling and convolutional layers configured to 2×2 and 3×3 filters, respectively. The CNN reached a testing accuracy (TA) of 100%. However, when the BS was changed to 128, the epochs adjusted to 30, with a softmax, the TA of CNN reached 98.99%. Therefore, the hyperparameter settings can improve the findings.

Table 6 presents the results of the proposed CNN model's performance utilizing the k-fold cross-validation method. In this approach, the dataset is split into five equal parts, where four are used for training and one for validation. The value of k, representing the number of partitions, is set to 5 in this case. The CNN model undergoes training five times, each with a different partition of the dataset. Based on this method, the CNN achieved a mean accuracy of 99.98% with a standard deviation of ±0.02%. The mean precision was 99.97% with a ±0.03% standard deviation, the average recall was 99.99% with a ±0.01% standard deviation, and the average F1-score reached 99.98% with a standard deviation of ±0.02%. These results demonstrate that the CNN model exhibits strong performance with minimal variability, and the use of k -fold cross-validation has further enhanced the model's effectiveness.

TABLE 6. The performance of the CNN model using 5-Fold cross-validation.

Metrics	CNN
Average Accuracy	99.98% (±0.02%)
Average Precision	99.97% (±0.03%)
Average Recall	99.99% (±0.01%)
Average $F1$-score	99.98% (±0.02%)

TABLE 7. The accuracy of the proposed CNN compared to other models in previous studies.

Reference	Model	Accuracy%	SNR in dB
[20]	CNN (1D phase-related feature)	99	0
[21]	Decision Tree with HOCs	88	-5
[22]	VB-DCNN	99.2	0
[23]	SCGNet	95.5	+ 30
[24]	FiF-Net	87	0
[26]	Modified CNN	96	+ 20
[31]	SCFNet	95	0
This Work	**CNN**	**100**	**+ 30**

The results demonstrate that the CNN model exhibits high accuracy and minimal loss rates during both testing and training phases. The PR curves, NCM, and ROC curves further validate that the CNN model accurately classifies modulation types. Figure 8 highlights the model's accuracy based on a dataset of 626 simulated images, while Figure 9 illustrates the model's performance in terms of a loss rate of 1.82×10^{-6}.

Figures 10 and 11 show the loss rate distributions for the two classes, highlighting the model's strong performance. Table 4 provides a classification report for the proposed model, where the F1 score, Recall, and Precision are all 100%. Additionally, the micro-average area under the PR curve is 100%, and the ROC curve for both classes also achieved 100% area, reflecting the model's exceptionally high performance.

Table 7 provides a comparison of the accuracy achieved in this study with previously published studies. It is clear that the 100% accuracy attained by the CNN surpasses that of the other models [20], [21], [22], [23], [24], [26], [31].

VII. CONCLUSION

This study highlights the effectiveness of CNNs for modulation recognition in underwater OWC systems. The proposed CNN model significantly outperforms traditional methods in recognizing 64-QAM and 32-PSK modulation schemes. By leveraging deep learning, we can enhance the reliability and accuracy of OWC systems for IoUT applications. The CNN was tested on a dataset consisting of 313 images each of 64QAM and 32PSK modulation schemes. The experiment demonstrated a perfect accuracy of 100% with a minimal test loss rate of 1.82×10^{-6}. Various assessing metrics were utilized to measure the model's performance, revealing a precision metric of 100%, a recall of 100%, and an F1-score of 100%.

The PR curves for the CNN showed a 100% area under the curve for both 64QAM and 32PSK classes. Similarly, the ROC curve also achieved an AUC of 100% for both classes. The hyperparameters settings of the CNN, including the loss and activation functions, significantly influenced the precision of the results. Optimal performance is contingent upon fine-tuning these parameters to achieve the best settings.

The performance of the CNN is also assessed based on precision, accuracy, F1-score, and recall utilizing the k-fold cross-validation method.

Therefore, referring to the proposed UOWC system, it presents distinct benefits compared to traditional acoustic and RF technologies in underwater settings. Additionally, it supports higher bandwidth and more reliable, high-speed communication, making it well-suited for data-intensive tasks like video streaming and advanced sensor networks. These advantages position UOWC as an efficient and high-performance solution for underwater communication.

The used dataset and developed code are available online at: https://www.kaggle.com/datasets/drsaeedmohsen/code-and-dataset.

VIII. FUTURE WORK

Future research will focus on extending the CNN model to handle additional modulation schemes and real-world underwater conditions. Exploring advanced deep learning techniques and integrating the model into practical communication systems will further enhance its applicability and performance. Also, one could apply the CNN model on different types of modulations. Additionally, one could develop a hybrid communication system that combine optical with RF or acoustic methods to extend the communication range and overcome absorption and scattering challenges.

The following points outline the practical implementation of the proposed CNN model in real-world IoUT applications, providing a clearer pathway for implementation in future systems. Several key challenges and requirements could be considered in the future work:

- Hardware Requirements: The implementation of the CNN model in real-world IoUT systems would require efficient hardware capable of handling the computational complexity of deep learning algorithms. Specifically, devices such as edge processors, GPUs, or specialized hardware accelerators (e.g., FPGAs or ASICs) would be necessary to perform real-time modulation classification without significantly increasing system latency. The selection of hardware would depend on the specific IoUT application, with trade-offs between power consumption, processing speed, and size being critical factors.
- Real-Time Performance: Ensuring real-time performance is essential for IoUT systems, particularly in time-sensitive applications such as underwater navigation or disaster monitoring. The proposed CNN model has been designed with an emphasis on fast inference times, making it suitable for real-time classification. In practice, the integration of low-latency data pipelines and optimized deep learning libraries (such as TensorRT or OpenVINO) would be essential to minimize the delay from data acquisition to modulation recognition.
- Environmental Considerations: IoUT systems often operate in challenging underwater environments with variable noise levels, signal attenuation, and limited bandwidth. Our model has been tested under a variety of simulated conditions to account for these factors, and we anticipate that adaptive real-time optimization, such as dynamically adjusting processing power based on environmental conditions, could be implemented to further improve system performance in practical deployments.
- Power Efficiency: Given that IoUT devices are often deployed in remote underwater locations with limited access to power sources, energy efficiency is a significant concern. The proposed CNN model's complexity can be adjusted by tuning the number of layers and neurons, allowing for a balance between accuracy and power consumption. We have also explored the potential for model compression techniques, such as pruning and quantization, to reduce power usage without sacrificing significant classification performance.

CONFLICT OF INTEREST

All authors have no conflict of interest regarding the publication of this paper.

ACKNOWLEDGMENT

The authors would like to thank Wael M. F. Abdel-Rehim for their support that helped conduct this study.

REFERENCES

[1] S. A. H. Mohsan, Y. Li, M. Sadiq, J. Liang, and M. A. Khan, "Recent advances, future trends, applications and challenges of Internet of Underwater Things (IoUT): A comprehensive review," *J. Mar. Sci. Eng.*, vol. 11, no. 1, p. 124, Jan. 2023.

[2] S. Mohsen, "A solar energy harvester for a wireless sensor system toward environmental monitoring," *Proc. Eng. Technol. Innov.*, vol. 21, pp. 10–19, Apr. 2022.

[3] C.-C. Kao, Y.-S. Lin, G.-D. Wu, and C.-J. Huang, "A comprehensive study on the Internet of Underwater Things: Applications, challenges, and channel models," *Sensors*, vol. 17, no. 7, p. 1477, Jun. 2017.

[4] M. F. Ali, D. N. K. Jayakody, Y. A. Chursin, S. Affes, and S. Dmitry, "Recent advances and future directions on underwater wireless communications," *Arch. Comput. Methods Eng.*, vol. 27, no. 5, pp. 1379–1412, Nov. 2020.

[5] S. Al-Zhrani, "Underwater optical communications: A brief overview and recent developments," *Engineered Sci.*, vol. 16, pp. 146–186, Jan. 2021.

[6] F. Zhang, C. Luo, J. Xu, and Y. Luo, "An efficient deep learning model for automatic modulation recognition based on parameter estimation and transformation," *IEEE Commun. Lett.*, vol. 25, no. 10, pp. 3287–3290, Oct. 2021.

[7] W. Zhang, K. Xue, A. Yao, and Y. Sun, "CTRNet: An automatic modulation recognition based on transformer-CNN neural network," *Electronics*, vol. 13, no. 17, p. 3408, Aug. 2024.

[8] Y. Qu, Z. Lu, R. Zeng, J. Wang, and J. Wang, "Enhancing automatic modulation recognition through robust global feature extraction," 2024, *arXiv:2401.01056*.

[9] M. Leblebici, A. Çalhan, and M. Cicioğlu, "CNN-based automatic modulation recognition for index modulation systems," *Expert Syst. Appl.*, vol. 240, Apr. 2024, Art. no. 122665.

[10] M. A. Abdel-Moneim, W. El-Shafai, N. Abdel-Salam, E. M. El-Rabaie, and F. E. A. El-Samie, "A survey of traditional and advanced automatic modulation classification techniques, challenges, and some novel trends," *Int. J. Commun. Syst.*, vol. 34, no. 10, pp. 1–36, Jul. 2021.

[11] A. Patil and M. Rane, "Convolutional neural networks: An overview and its applications in pattern recognition," in *Proc. Int. Conf. Inf. Commun. Technol. Intell. Syst.*, vol. 1, 2021, pp. 21–30.

[12] Z. Li, F. Liu, W. Yang, S. Peng, and J. Zhou, "A survey of convolutional neural networks: Analysis, applications, and prospects," *IEEE Trans. Neural Netw. Learn. Syst.*, vol. 33, no. 12, pp. 6999–7019, Dec. 2022.

[13] Y. Liu, H. Pu, and D.-W. Sun, "Efficient extraction of deep image features using convolutional neural network (CNN) for applications in detecting and analysing complex food matrices," *Trends Food Sci. Technol.*, vol. 113, pp. 193–204, Jul. 2021.

[14] R. Zhou, F. Liu, and C. W. Gravelle, "Deep learning for modulation recognition: A survey with a demonstration," *IEEE Access*, vol. 8, pp. 67366–67376, 2020.

[15] B. Jdid, K. Hassan, I. Dayoub, W. H. Lim, and M. Mokayef, "Machine learning based automatic modulation recognition for wireless communications: A comprehensive survey," *IEEE Access*, vol. 9, pp. 57851–57873, 2021.

[16] D. Menaka, S. Gauni, C. T. Manimegalai, and K. Kalimuthu, "Vision of IoUT: Advances and future trends in optical wireless communication," *J. Opt.*, vol. 50, no. 3, pp. 439–452, Sep. 2021.

[17] S. A. H. Mohsan, A. Mazinani, H. B. Sadiq, and H. Amjad, "A survey of optical wireless technologies: Practical considerations, impairments, security issues and future research directions," *Opt. Quantum Electron.*, vol. 54, no. 3, p. 187, Mar. 2022.

[18] X. Sun, C. H. Kang, M. Kong, O. Alkhazragi, Y. Guo, M. Ouhssain, Y. Weng, B. H. Jones, T. K. Ng, and B. S. Ooi, "A review on practical considerations and solutions in underwater wireless optical communication," *J. Lightw. Technol.*, vol. 38, no. 2, pp. 421–431, Jan. 2020.

[19] D. S. Chauhan, G. Kaur, and D. Kumar, "Deep learning based modulation classification for underwater optical wireless communication system," in *Proc. Int. Conf. Emerg. Res. Comput. Sci. (ICERCS)*, Dec. 2023, pp. 1–6.

[20] W. Xu, Y. Wang, F. Wang, and X. Chen, "PSK/QAM modulation recognition by convolutional neural network," in *Proc. IEEE/CIC Int. Conf. Commun. China (ICCC)*, Oct. 2017, pp. 1–5.

[21] A. K. Ali and E. Erçelebi, "Algorithm for automatic recognition of PSK and QAM with unique classifier based on features and threshold levels," *ISA Trans.*, vol. 102, pp. 173–192, Jul. 2020.

[22] M. Talha, M. Sarfraz, A. Rahman, S. A. Ghauri, R. M. Mohammad, G. Krishnasamy, and M. Alkharraa, "Voting-based deep convolutional neural networks (VB-DCNNs) for M-QAM and M-PSK signals classification," *Electronics*, vol. 12, no. 8, p. 1913, Apr. 2023.
[23] G. B. Tunze, T. Huynh-The, J.-M. Lee, and D.-S. Kim, "Sparsely connected CNN for efficient automatic modulation recognition," *IEEE Trans. Veh. Technol.*, vol. 69, no. 12, pp. 15557–15568, Dec. 2020.
[24] V.-S. Doan, T. Huynh-The, C.-H. Hua, Q.-V. Pham, and D.-S. Kim, "Learning constellation map with deep CNN for accurate modulation recognition," in *Proc. GLOBECOM IEEE Global Commun. Conf.*, Dec. 2020, pp. 1–6.
[25] S. Lee, Y.-I. Yoon, and Y. J. Jung, "Generative adversarial network-based signal inpainting for automatic modulation classification," *IEEE Access*, vol. 11, pp. 50431–50446, 2023.
[26] O. N. M. Salim, S. A. Adnan, and A. H. Mutlag, "Underwater optical wireless communication system performance improvement using convolutional neural networks," *AIP Adv.*, vol. 13, no. 4, pp. 1–11, Apr. 2023.
[27] Y. Wang, H. Zhang, Z. Sang, L. Xu, C. Cao, and T. A. Gulliver, "Modulation classification of underwater communication with deep learning network," *Comput. Intell. Neurosci.*, vol. 2019, pp. 1–12, Apr. 2019.
[28] W. Xiao, Z. Luo, and Q. Hu, "A review of research on signal modulation recognition based on deep learning," *Electronics*, vol. 11, no. 17, p. 2764, Sep. 2022.
[29] F. Zhang, C. Luo, J. Xu, Y. Luo, and F.-C. Zheng, "Deep learning based automatic modulation recognition: Models, datasets, and challenges," *Digit. Signal Process.*, vol. 129, Sep. 2022, Art. no. 103650.
[30] M. K. Younis, M. A. Al-Mousawi, and Y. W. Kwon, "Signal classification using deep learning techniques: Review and future directions," *Artif. Intell. Rev.*, vol. 56, no. 3, pp. 2437–2470, 2023.
[31] H. Han, Z. Yi, Z. Zhu, L. Li, S. Gong, B. Li, and M. Wang, "Automatic modulation recognition based on deep-learning features fusion of signal and constellation diagram," *Electronics*, vol. 12, no. 3, p. 552, Jan. 2023.
[32] S. Peng, H. Jiang, H. Wang, H. Alwageed, and Y.-D. Yao, "Modulation classification using convolutional neural network based deep learning model," in *Proc. 26th Wireless Opt. Commun. Conf. (WOCC)*, Apr. 2017, pp. 1–5.
[33] Y. Zeng, M. Zhang, F. Han, Y. Gong, and J. Zhang, "Spectrum analysis and convolutional neural network for automatic modulation recognition," *IEEE Wireless Commun. Lett.*, vol. 8, no. 3, pp. 929–932, Jun. 2019.
[34] Y. Xu, D. Li, Z. Wang, Q. Guo, and W. Xiang, "A deep learning method based on convolutional neural network for automatic modulation classification of wireless signals," *Wireless Netw.*, vol. 25, no. 7, pp. 3735–3746, Oct. 2019.
[35] H. S. Ghanem, R. M. Al-Makhlasawy, W. El-Shafai, M. Elsabrouty, H. F. A. Hamed, G. M. Salama, and F. E. A. El-Samie, "Wireless modulation classification based on radon transform and convolutional neural networks," *J. Ambient Intell. Humanized Comput.*, vol. 14, no. 5, pp. 6263–6272, May 2023.
[36] S. Mohsen, A. M. Ali, and A. Emam, "Automatic modulation recognition using CNN deep learning models," *Multimedia Tools Appl.*, vol. 83, no. 3, pp. 7035–7056, Jan. 2024.
[37] E. Felemban, F. K. Shaikh, U. M. Qureshi, A. A. Sheikh, and S. B. Qaisar, "Underwater sensor network applications: A comprehensive survey," *Int. J. Distrib. Sensor Netw.*, vol. 11, no. 11, Nov. 2015, Art. no. 896832.
[38] K. A. U. Menon, D. P, and M. V. Ramesh, "Wireless sensor network for river water quality monitoring in India," in *Proc. 3rd Int. Conf. Comput., Commun. Netw. Technol. (ICCCNT)*, Jul. 2012, pp. 1–7.
[39] H. Saeed, S. Ali, S. Rashid, S. Qaisar, and E. Felemban, "Reliable monitoring of oil and gas pipelines using wireless sensor network (WSN)—REMONG," in *Proc. 9th Int. Conf. Syst. Syst. Eng. (SOSE)*, Jun. 2014, pp. 230–235.
[40] A. Khan and L. Jenkins, "Undersea wireless sensor network for ocean pollution prevention," in *Proc. 3rd Int. Conf. Commun. Syst. Softw. Middleware Workshops (COMSWARE)*, Jan. 2008, pp. 2–8.
[41] C. Alippi, R. Camplani, C. Galperti, and M. Roveri, "A robust, adaptive, solar-powered WSN framework for aquatic environmental monitoring," *IEEE Sensors J.*, vol. 11, no. 1, pp. 45–55, Jan. 2011.
[42] A. Davis and H. Chang, "Underwater wireless sensor networks," in *Proc. Oceans*, Oct. 2012, pp. 1–5.
[43] S. Srinivas, P. Ranjitha, R. Ramya, and G. K. Narendra, "Investigation of oceanic environment using large-scale UWSN and UANETs," in *Proc. 8th Int. Conf. Wireless Commun., Netw. Mobile Comput.*, Sep. 2012, pp. 1–5.
[44] S. Bainbridge, D. Eggeling, and G. Page, "Lessons from the field—Two years of deploying operational wireless sensor networks on the great barrier reef," *Sensors*, vol. 11, no. 7, pp. 6842–6855, Jun. 2011.
[45] R. Marin-Perez, J. García-Pintado, and A. S. Gómez, "A real-time measurement system for long-life flood monitoring and warning applications," *Sensors*, vol. 12, no. 4, pp. 4213–4236, Mar. 2012.
[46] P. Kumar, P. Kumar, P. Priyadarshini, and Srija, "Underwater acoustic sensor network for early warning generation," in *Proc. Oceans*, Oct. 2012, pp. 1–6.
[47] K. Casey, A. Lim, and G. Dozier, "A sensor network architecture for tsunami detection and response," *Int. J. Distrib. Sensor Netw.*, vol. 4, no. 1, pp. 27–42, Jan. 2008.
[48] R. B. Manjula and S. S. Manvi, "Coverage optimization based sensor deployment by using PSO for anti-submarine detection in UWASNs," in *Proc. Ocean Electron. (SYMPOL)*, Oct. 2013, pp. 15–22.
[49] S. Khaledi, H. Mann, J. Perkovich, and S. Zayed, "Design of an underwater mine detection system," in *Proc. Syst. Inf. Eng. Design Symp. (SIEDS)*, Apr. 2014, pp. 78–83.
[50] E. Cayirci, H. Tezcan, Y. Dogan, and V. Coskun, "Wireless sensor networks for underwater surveillance systems," *Ad Hoc Netw.*, vol. 4, no. 4, pp. 431–446, 2006.
[51] F. A. D. Magalhaes, G. Vannozzi, G. Gatta, and S. Fantozzi, "Wearable inertial sensors in swimming motion analysis: A systematic review," *J. Sports Sci.*, vol. 33, no. 7, pp. 732–745, Apr. 2015.
[52] M. Waldmeyer, H.-P. Tan, and W. K. G. Seah, "Multi-stage AUV-aided localization for underwater wireless sensor networks," in *Proc. IEEE Workshops Int. Conf. Adv. Inf. Netw. Appl.*, Mar. 2011, pp. 908–913.
[53] Y. Guo and Y. Liu, "Localization for anchor-free underwater sensor networks," *Comput. Electr. Eng.*, vol. 39, no. 6, pp. 1812–1821, Aug. 2013.
[54] M. M. Zayed, M. Shokair, S. Elagooz, and H. Elshenawy, "A more detailed mathematical model for analyzing the link budget in UWOCs for both LoS and N-LoS scenarios," *J. Opt.*, pp. 1–29, Sep. 2024. [Online]. Available: https://link.springer.com/article/10.1007/s12596-024-02220-2#citeas
[55] M. M. Zayed, M. Shokair, S. Elagooz, and H. Elshenawy, "Link budget analysis of LED-based UWOCs utilizing the optimum Lambertian order (OLO)," *Opt. Quantum Electron.*, vol. 56, no. 9, pp. 1–28, Aug. 2024.
[56] M. M. Zayed, M. Shokair, S. Elagooz, and H. Elshenawy, "Feasibility analysis of line of sight (LOS) underwater wireless optical communications (UWOCs) via link budget," *Opt. Quantum Electron.*, vol. 56, no. 6, p. 1012, May 2024.
[57] M. M. Zayed, M. Shokair, S. Elagooz, and H. Elshenawy, "Non-line-of-sight (NLOS) link budget analysis for underwater wireless optical communications (UWOCs)," *Opt. Quantum Electron.*, vol. 56, no. 7, p. 1206, Jun. 2024.
[58] (2024). *Radio-Modulation-Dataset, Kaggle Repository*. [Online]. Available: https://www.kaggle.com/datasets/drsaeedmohsen/radio-modulation-types-dataset

M. MOKHTAR ZAYED received the B.Sc. degree (Hons.) in communication and computer engineering from the Higher Institute of Engineering, Elshorouk Academy, Al Shorouk City, Cairo, Egypt, in 2013, and the M.Sc. degree in electrical engineering from the Department of Electronics and Electrical Communications, Faculty of Engineering, Ain Shams University, Cairo, in 2019. He is currently pursuing the Ph.D. degree with the Department of Electronics and Electrical Communications, Faculty of Electronic Engineering, Menoufia University. He is currently a Lecturer Assistant with the Department of Communication and Computer Engineering, Elshorouk Higher Institute of Engineering, Cairo. His research interests include optical wireless communication (OWC), the Internet of Underwater Things (IoUT), underwater communications, underwater applications, the Internet of Things (IoT), mobile communications, satellite communications, wireless communications, digital signal processing (DSP), random signals and noise, digital communications, signal analysis, signal processing for communication, and digital communications.

SAEED MOHSEN received the B.Sc. degree (Hons.) in electronics engineering and electrical communications from Thebes Higher Institute, Cairo, Egypt, in 2013, and the M.Sc. and Ph.D. degrees in electrical engineering from Ain Shams University, Cairo, in 2016 and 2020, respectively. He is currently an Assistant Professor with the Al-Madinah Higher Institute for Engineering and Technology, Giza, Egypt. He made intensive research on applications of artificial intelligence (AI), such as deep learning, machine learning, and neural networks. He has published over 25 scientific papers in specialized international conferences and peer-reviewed periodicals. His research interests include biomedical engineering, wearable devices, energy harvesting, analog electronics, and the Internet of Things (IoT). He acts as a Reviewer of several scientific journals, such as IEEE Access and *IET Communications*.

ABDULLAH ALGHURIED received the Ph.D. degree in industrial engineering from the University of Miami, in 2020. He is currently an Assistant Professor in industrial engineering with the University of Tabuk. His research interests include stochastic modeling and optimization, data mining, big data, data analytics, decision-making under uncertainty, lean six sigma, and sustainability.

HASSAN HIJRY (Associate Member, IEEE) received the M.S. degree in industrial engineering from Lawrence Technological University (LTU) and the Ph.D. degree in systems engineering from Oakland University, USA. He is currently an Assistant Professor in industrial engineering with the University of Tabuk, Saudi Arabia. He brings industry experience as a Former Front-Line Manager of PEPSICO, Riyadh. His teaching expertise spans work study, production planning and control, facilities planning, materials handling, and industry 4.0 technologies and engineering management. His research interests include industry x.0, AI, ML within diverse sectors like workplaces, manufacturing industries, and healthcare systems.

MONA SHOKAIR received the B.E. and M.Sc. degrees in electronics engineering from El-Menoufia University, El-Menoufia, Egypt, in 1993 and 1997, respectively, and the Ph.D. degree from Kyushu University, Japan, in 2005. From 2005 to 2010, she was a Lecturer with El-Menoufia University, where she was an Associate Professor, from 2011 to 2015. She was the Head of the Electronic and Communication Department, Faculty of Engineering, from 2016 to 2019. She was the Vice Dean of Postgraduate, from 2019 to 2022. She is currently the Head of the Electrical Engineering Department, Faculty of Engineering, October 6 University. She received a lot of awards, such as VTS chapter IEEE Award from Japan, in 2003. She received Best Paper from NRSC 2016. She has published over 210 articles. She is also working in OFDM systems, LTE-cognitive radio, WiMAX, cellular communication, communication system & signal processing, electronics, GSM, channel estimation, mobile communications, resource allocation, coding, radio propagation, WIMAX systems, and D2D systems.